Multitone Frequency-Domain Simulation of Nonlinear Circuits in Large- and Small-Signal Regimes

Nuno Borges de Carvalho, *Student Member, IEEE,* and José Carlos Pedro, *Member, IEEE*

***Abstract*—Computer simulation of general microwave nonlinear circuits excited by a large number of input tones is addressed. The algorithm, based on the spectral-balance method, uses novel index-vector and convolution-matrix generation techniques. That, in conjunction with a new nonlinear-device modeling approach (which directly takes into account the higher order derivatives of the I/V and Q/V characteristics), allowed the prediction of such complex behavior as spectral regrowth and noise–power ratio (NPR) tests of a class-B power amplifier or multitone intermodulation phenomena in a saturated multioctave amplifier.**

***Index Terms*— Computer-aided analysis, frequency-domain analysis, nonlinear circuits, nonlinear distortion.**

I. Introduction

RECENT advances in telecommunications systems, particularly broad-band services and mobile networks, continuously present new challenges to microwave computer-aided design (CAD) tools. On one hand, to achieve higher output power and efficiency, amplifier circuits are being pushed to saturated classes of operation. While on the other hand, circuit-design linearity is permanently driven by improved system performance. Due to the complex nonlinear phenomena involved, microwave engineers no longer rely on the classic single-carrier or two-tone tests. Alternatively, they are seeking new characterization procedures like the observation of the spectral regrowth produced in a nonlinear circuit excited by a modulated carrier or even the identification of the newly generated spectral components when the circuit is expected to handle a very large number of input tones—the so-called noise–power ratio (NPR) test. Accompanying that scenario, an obvious need to incorporate prediction facilities of these experiments in today's microwave CAD simulation tools appeared. However, until now, the problem of simulating the response of a strong nonlinear circuit driven by a complex spectral signal in a digital computer was virtually unsolved. In fact, neither an efficient and reliable nonlinear analysis method is available, nor are the modeling procedures normally adopted for microwave electron devices sufficiently mature to accurately describe both small- and large-signal intermodulation distortion (IMD) behavior.

Manuscript received November 6, 1997; revised May 16, 1998. This work was supported by the JNICT under Doctoral Grant Praxis XXI/BD/5630/95 and by LIRA Project 2496/TIT/95.

The authors are with the Instituto de Telecomunicações, Universidade de Aveiro, 3810 Aveiro, Portugal (e-mail: nborges@av.it.pt; jcpedro@av.it.pt).

Publisher Item Identifier S 0018-9480(98)09041-3.

For what the analysis method is concerned with, both the time-domain (SPICE-like programs [1]) and the hybrid time-domain/frequency-domain-based packages (harmonic-balance (HB) programs [2]) cannot be directly applied.

The nonexistence of time-domain representations of some microwave components (e.g., dispersive transmission media or discontinuities) associated with the widely known long computer runs needed to find the steady-state regime of even the simplest microwave circuit gave SPICE a rapidly decreasing acceptance in the microwave design field.

This space was rapidly filled by HB, which proved itself an invaluable tool for predicting the nonlinear regime under single sinusoid excitation. However, when multitone operation is the objective, HB still presents many difficulties, which are mainly due to the required successive application of the discrete Fourier transform (DFT). Because of that, some exact alternatives (e.g., multidimensional Fourier transform (MDFT) [3], or approximate methods such as the almost-periodic Fourier transform (APFT) [4]) have been proposed, which are too heavy when the input signal is composed of more than two or three incommensurate tones.

Very recently, some hybrid alternatives based on the time-domain integration of the envelope baseband signal [envelope simulators (ES's)] [5], [6] were especially proposed to solve that kind of simulation problem. Since they were conceived to deal with single-modulated carrier excitations, they have been successfully applied to the simulation of spectral regrowth and narrow-band NPR, but they suffer from an inherent disadvantage: they are restricted to driving signals that occupy a small percentage of the nonlinear circuit's bandwidth. Therefore, they will not be useful in simulating responses of circuits where the available bandwidth is fully utilized. Also, due to their need to treat the circuit excitation as a carrier modulated by some time-domain baseband signal, they appear to be unable to handle practical input spectra, such as more than one modulated carrier.

From this brief overview, one can conclude that, at least these days, the best way to solve the problem of simulating nonlinear circuits driven by general multitone signals is to select one of the available analytical methods that operate entirely in the frequency domain: Volterra series [7] or frequency-domain HB: spectral balance (SB) [8].

Despite the many advantages presented by the Volterra series method, which makes it the ideal tool for simulating all types of small-signal intermodulation phenomena, it is

restricted to mild nonlinear regimes [9]. Thus, it is useless for predicting the nonlinear responses of any saturated circuit.

The SB algorithm is especially appropriate for this problem as it picks up the frequency representation of the excitation (the domain where it is normally perceived and best described in the microwave field) and provides an output in the same form. It performs all simulation steps without passing through time domain, thus obviating the need for any Fourier transform. However, it still presents some implementation problems, which prevent its spread. In this paper, we will start by making a review of the SB technique and then address some of its key points. Some new ideas to overcome this problems will then be proposed, which will enable the reliable application of the SB analysis technique to strong nonlinear circuits driven by multitone spectra.

The other nonlinear simulation issue that was mentioned at the beginning of this section was the adopted device modeling functional form. As is widely known, accurate prediction of IMD behavior requires electron-device-model descriptions that represent not only the I/V or Q/V characteristics, but also its higher order derivatives [10]. Also, SB implementations require that the device model has some polynomial (or rational function) form. Techniques usually followed to construct these mathematical approximants consist of a simple I/V and Q/V curve fitting. In the following sections a systematic procedure to determine an nth-order approximant that osculates with the function and its first n derivatives will also be discussed.

Finally, this paper presents various simulation scenarios of spectral regrowth, NPR, and multitone IMD, and compares simulated and experimental results of nonlinear multitone excitation regime obtained from a microwave class-B amplifier.

II. SB Revisited

The SB concept is similar to the well-known HB. As was already told, what distinguishes it from HB is the ability to calculate the circuit's response spectra entirely in the frequency domain. In fact, all functional steps of both algorithms are equal, except that no mapping of frequency and time domains is needed.

Since each of these steps is already well discussed in the literature [11]–[13], we will focus our attention on those that are more important to the SB.

The first of these is the generation of the mixed-frequency index vector. This index vector is essential to both the HB and SB algorithms because it will give the size and frequency position of the circuit unknowns. Furthermore, the size of this vector will determine the dimension of the Jacobian, which is the largest matrix involved in the algorithm.

In [14] and [15], the index vector was calculated using some nested loops and the following formula:

$$\omega_k = k_1\omega_1 + k_2\omega_2 + \cdots k_n\omega_n \tag{1}$$

where the harmonic number of $k_1, \cdots, k_n$ are integers, and $\omega_1, \cdots, \omega_n$ are the input frequencies of each excitation tone.

This way of calculating the index vector is very time consuming and can generate equal frequency positions in the ω_k vector. Therefore, some sorting algorithm is further needed to organize the vector and to exclude redundant frequencies. In Section III, a new way to calculate the index vector which overcomes these problems will be presented.

In SB, a convolution matrix is needed to perform time-domain multiplication's and divisions in the frequency domain. This problem has already been studied by Rhyne and Steer [14] and Närhi [15]. Steer used a mixed algorithm that includes a mapping function and an auxiliary routine, which creates the matrix [16]. Other authors [17] follow similar procedures when they use a mix of two or three algorithms to generate the convolution matrix. However, until now, no one had associated those techniques with the well-known linear convolution. Thus, a new way to generate the convolution matrix based on the linear convolution will also be presented in Section III.

The main idea under the SB algorithm consists of obtaining the current responses of the circuit's nonlinear elements to the applied control voltages, directly in the frequency domain. Therefore, any nonlinear active device model should be described by some basis functions for which spectra calculations are not a too difficult task. One way to select those basis functions is to simply rely on the elementary arithmetic operations since time-domain addiction and subtraction have a direct correspondent in the frequency domain and multiplication and division can be mapped to spectral convolution and deconvolution. That idea, originally introduced by Chang and Steer [18], and named the arithmetic operator method (AOM), requires that any model should be represented by a combination of these elementary operations. One way to do that is to use polynomial or rational functions as the selected model's approximant.

This type of restriction is not really specific to the SB method. In fact, when traditional time-domain models are used, complex functions are also evaluated using some kind of approximant decomposable in the four elementary arithmetic operations. The only difference is that, there, the fitting process (usually a decomposition in continued fraction expansions) is implicit since it is embedded in the computer.

Steer [8] used a generalized power series as the approximation process, but the development was too complex. In [19], Steer uses a more general algebraic analytical form. Närhi [17] considers the nonlinearity as a black box and approximates it using Chebyshev polynomials/rationals that are more robust to strong nonlinearities. Eijnde [20], [21] uses a rational approximant, which is derived using minimum squares fitting in order to represent strong nonlinearities with fewer terms.

All of these approximants need only information of the I/V or Q/V curves, providing no control of the functions' higher order derivatives.

Since it is now perfectly understood that the model's higher order derivatives determine the generation of intermodulation products [10], a new type of approximant, the Hermite rational, conceived to accurately represent the function and its first n derivatives, will be presented in Section IV.

TABLE I
OUTPUT INDEX VECTOR GENERATED BY THREE TONES MIXED UP TO FIFTH ORDER

0	0.001	0.002	0.003	0.004						
.996	.997	.998	.999	1	**1.001**	1.002	1.003	1.004	1.005	1.006
1.998	1.999	2	2.001	**2.002**	2.003	2.004	2.005	2.006		
2.998	2.999	3	3.001	3.002	**3.003**	3.004	3.005	3.006	3.007	3.008
4	4.001	4.002	4.003	**4.004**	4.005	4.006	4.007	4.008		
5	5.001	5.002	5.003	5.004	**5.005**	5.006	5.007	5.008	5.009	5.010

III. NEW INDEX TECHNIQUE AND CONVOLUTION MATRIX

A. Index-Vector Generation

If the input-signal spectrum can be considered as regular (such as the one previously used by Ngoya and Obregon [22], and redefined here as $\omega_k = \omega_0 + k\Delta\omega$, where ω_k is the input frequencies, ω_0 is the first component, and $\Delta\omega$ is the frequency step), we found that it is possible to determine the whole mixing vector using only very simple formulas.

To exemplify, let us consider an input-signal spectrum composed of three tones: 1, 1.001, and 1.002 GHz, and a sought output simulation result until the fifth mixing order. The positive part of the index vector is represented in Table I, where the output frequency components were distributed in rows in ascending order.

By inspection, one can easily conclude that the resulting spectrum may be interpreted as being constituted of six narrow-band groups of tones, regularly separated by $\Delta\omega$ (plus their negative counterparts), centered at dc—0 Hz, ω_1—1.001 GHz, $2.\omega_1$—2.002 GHz, $3.\omega_1$—3.003 GHz, $4.\omega_1$—4.004 GHz, $5.\omega_1$—5.005 GHz, and having the following widths or number of tones each: dc—9, ω_1—11, $2.\omega_1$—9, $3.\omega_1$—11, $4.\omega_1$—9, and at $5.\omega_1$—11.

In general, it was found that the central mixing frequencies could be obtained by

$$f_{\text{central}} = \begin{cases} \left(\frac{f_m + f_{m+1}}{2}\right) \cdot c, & \text{if number of tones is even} \\ f_m \cdot c, & \text{if number of tones is odd} \end{cases} \tag{2}$$

with f_m and f_{m+1} the input central frequencies and $\mathbf{c}$ the nonlinear order; while the correspondent spectral widths located around the central frequency f_{central} may be calculated from

$$\text{number of newly generated tones} = C_{o,e}.n - (C_{o,e} - 1) \tag{3}$$

with $\mathbf{n}$ the number of original tones, and $C_{o,e}$ the maximum even or odd order for even or odd harmonics, respectively, as can be easily observed from Table I.

Further using the input spectrum regularity, it can also be easily observed from Table I that it is only necessary to calculate the spectral widths for the maximum order of c and $c-1$ because lower orders of equal parity have the same spectral width.

With this type of closed formulation, the latter problems presented in Section II were resolved. In fact, it is now possible to generate the index vector using only approximate $(n-1)C^2 + C + 1$ steps, where (C is $\max(C_{o,e})$), instead of the $(2C+1)^n$ steps required by the previous technique of Steer and Närhi [14], [15]. For the example depicted in Table I ($n = 3$ and $c = 5$), only 90 loops were sufficient to determine the whole index vector, against the 1331 loops that would be required by the previous techniques. The difference has a fast increase as n grows.

In addition, the present formulation obviates the referred need to use some kind of sorting algorithm, as it does not produce any distinct vector positions of equal frequency. Therefore, significant amounts of simulation time and memory requirements for saving the convolution and Jacobian matrices may be earned, compared to other commercially available HB implementations like MDS.[1]

Although those benefits were, in fact, a direct consequence of the considered input spectrum symmetry, it will be shown later that this kind of excitation is quite suitable for representing a lot of real telecommunication signals, like the ones encountered in frequency mixers, uniformly discretized continuous spectra, and pseudorandom sequences used in digital circuits.

B. Convolution-Matrix Generation

For better understanding the convolution-matrix generation process now proposed, let us consider the usual linear convolution formula

$$a(j) = \sum_{i=-N}^{N} y(i)x(j-i) \tag{4}$$

where N is the number of samples, Y and X are the convolution sampled vector operands, and A is the result: $A = Y*X$. If, for illustration purposes, 13 samples are chosen and $X = Y = [000j^*j^*000jj000]$, (4) can be put into a graphic form, as shown in Table II. It can be seen that the numbers between the slashed lines constitute the so-called X associated convolution matrix T_x defined by $YT_x = A$.

Consider now that two equal spectral vectors X and Y must be convolved. Each vector has an associated mixed-frequency index vector, which is generated using the technique explained above. If, for simplicity, a two-tone spectrum is under consideration, then the input frequency-component positions and their values can be seen in Table III.

The convolution of X^*Y will be done using the same graphical procedure used for the linear convolution. Since the amplitude vector is equal to the one previously considered (see Table II), the amplitude convolution matrix is also equal, but now, different mixing frequencies will appear. Thus, if

[1] MDS, HP 85150B Microwave and RF Design Systems, Hewlett-Packard Company, Santa Rosa, CA, 1994.

TABLE II
GRAPHICAL LINEAR CONVOLUTION PROCEDURE

y→	0	0	0	j*	j*	0	0	0	j	j	0	0	0	a↓
x→	0													0
x→	0	0												0
x→	0	0	0											0
x→	J*	0	0	0										0
x→	j*	j*	0	0	0									0
x→	0	j*	j*	0	0	0								0
x→	0	0	j*	j*	0	0	0							-1
x→	0	0	0	j*	j*	0	0	0						-2
x→	j	0	0	0	j*	j*	0	0	0					-1
x→	j	j	0	0	0	j*	j*	0	0	0				0
x→	0	j	j	0	0	0	j*	j*	0	0	0			0
x→	0	0	j	j	0	0	0	j*	j*	0	0	0		2
x→	0	0	0	j	j	0	0	0	j*	j*	0	0	0	4
x→		0	0	0	j	j	0	0	0	j*	j*	0	0	2
x→			0	0	0	j	j	0	0	0	j*	j*	0	0
x→				0	0	0	j	j	0	0	0	j*	j*	0
x→					0	0	0	j	j	0	0	0	j*	-1
x→						0	0	0	0	j	j	0	0	-2
x→							0	0	0	0	j	j	0	-1
x→								0	0	0	j	j	0	0
x→									0	0	0	j	j	0
x→										0	0	0	j	0
x→											0	0	0	0
x→												0	0	0
x→													0	0

TABLE III
INPUT FREQUENCY VECTOR

X=Y=

$-2f_2$	$-f_2-f_1$	$-2f_1$	$-f_2$	$-f_1$	f_1-f_2	0	f_2-f_1	f_1	f_2	$2f_1$	f_1+f_2	$2f_2$
0	0	0	j*	j*	0	0	0	j	j	0	0	0

TABLE IV
SAMPLE COMPONENTS OF THE FREQUENCY CONVOLUTION MATRIX

	$-2f_2$	$-f_2-f_1$	$-2f_1$	$-f_2$	$-f_1$	...	
j=7	0	f_1-f_2	$-f_1$	$-f_2$	$-2f_1$	...	$-2f_2;-3f_1$
j=8	f_2-f_1	0	f_1-f_2	$-f_1$	$-f_2$	...	$-f_2-f_1$
j=9	f_1	f_2-f_1	0	f_1-f_2	$-f_1$	...	$f_1-2f_2;-2f_1$
j=10	f_2	f_1	f_2-f_1	0	f_1-f_2	...	$-f_2;-3f_1+f_2$

the convolution is done on the frequency vector, the resulting frequency components can be obtained as the samples represented in Table IV.

In the right column of Table IV, there are some mixing components that have orders greater than two, which do not belong to the mixing-frequency index vector. Thus, it is obvious that these unwanted mixing frequencies must be ignored, both on the amplitude and frequency convolution matrix.

One problem that arises from this kind of algorithm is the use of the entire spectrum, positive and negative, which represents some wasted time when dealing with real signals. The way proposed here to overcome this is to ignore the first lines of the convolution matrix (correspondent to the output negative spectrum) and then mirror the negative part onto the positive part. The size of the resulting matrix is equal to the size of the shaded block shown in Table II.

IV. HERMITE RATIONALS

As already mentioned in Section II, to apply the SB algorithm to a nonlinear device, a polynomial and/or a rational function must be used as the nonlinear model. There, the state-of-art in approximants appropriate for SB implementations was reviewed. We will now present a new type of approximant that is more suitable for IMD studies.

As is known [20], when strong nonlinearities are to be approximated, rational functions are better then polynomials because of their increased range of convergence for the same number of terms. Thus, a rational approximant must be sought. Furthermore, since the model's derivatives play a dominant role in IMD calculations [10], the approximant must also accurately represent not only the function, but its derivatives as well.

A suitable approximant that verifies both conditions is the Hermite rational [23]. Beyond its rational form, being a Hermite, means that the approximation osculates with the function in the n first derivatives.

Skipping most of the mathematical parts, described in detail on [23], we will present the basis and methods to approximate any function by a Hermite rational.

Consider that a function $f(x)$ and all its derivatives are known. The Hermite rational consists of calculating the following polynomials:

$$p(x)=\sum_{i=0}^{m} a_i x^i \quad \text{and} \quad q(x)=\sum_{i=0}^{n} b_i x^i \tag{5}$$

so that they verify the condition

$$\begin{cases} f^{(\ell)}(x_i)=\left(\dfrac{p}{q}\right)^{(\ell)}, & (x_i) \text{ and } \ell=0,\cdots,s_i-1, \\ & \text{with } i=0,\cdots,j \\ f^{(\ell)}(x_{j+1})=\left(\dfrac{p}{q}\right)^{(\ell)}, & (x_{j+1}) \text{ and } \ell=0,\cdots,k-1. \end{cases} \tag{6}$$

One of the Hermite rational forms is the continued fraction expansion of Thiele [23]

$$f(x)=\varphi_0(x_0)+\cfrac{x-x_0}{\varphi_1(x_0)+\cfrac{x-x_1}{\varphi_2(x_0)+\cdots}}. \tag{7}$$

Using Thiele's method, we have

$$\begin{aligned} \varphi_0(x)&=f(x) \\ \varphi_1(x)&=\frac{1}{f'(x)} \\ \varphi_j&=j\left(\frac{\partial \rho_{j-1}(x)}{dx}\right)^{-1} \\ \rho_j(x)&=\rho_{j-2}(x)+\varphi_j(x) \\ \rho_0(x)&=\varphi_0(x). \end{aligned} \tag{8, 9}$$

Since Hermite rationals can be constructed from data in analytical or tabular form, any kind of tabular model extracted

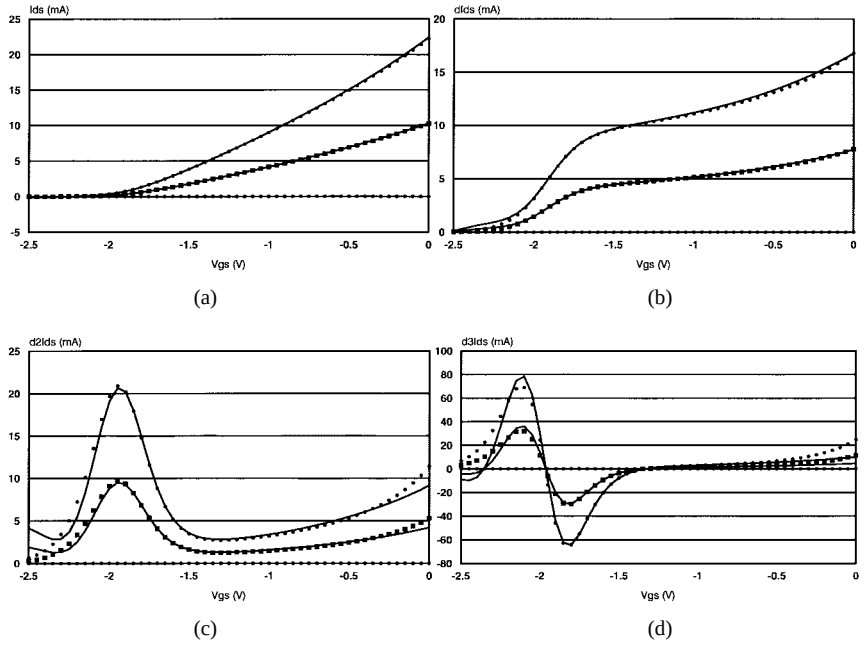

Fig. 1. (a) $I_{\rm ds}$ versus $V_{\rm gs}$. (b) First derivative, (c) second derivative, and (d) third derivative for linear region ($V_{\rm DS} = 0$ V and $V_{\rm DS} = 0.5$ V) and saturation ($V_{\rm DS} = 5$ V).

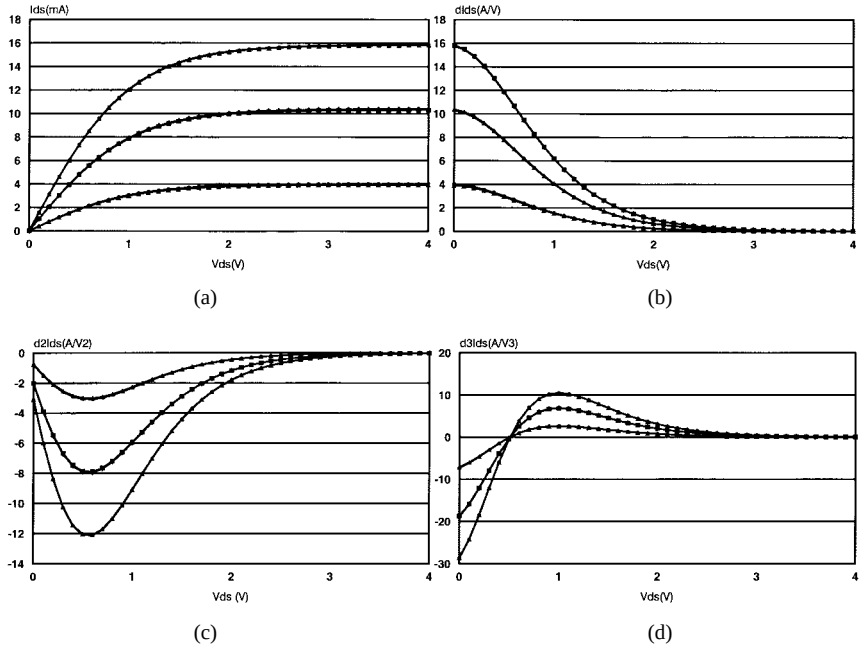

Fig. 2. (a) $I_{\rm ds}$ versus $V_{\rm ds}$. (b) First derivative, (c) second derivative, and (d) third derivative, for three different $V_{\rm GS}$ bias points $V_{\rm GS} = 0$ V, $V_{\rm GS} = -0.5$ V and $V_{\rm GS} = -1$ V.

from measurements can also be approximated. By generalizing this concept, it is also possible to determine Hermite rationals of multivariate functions [24].

In order to exemplify the technique just explained, an in-house developed MESFET model [25] will now be approximated using Hermite rationals.

The major devices of nonlinear behavior herein considered are: the drain–source current $I_{\rm ds}(V_{\rm gs}, V_{\rm ds})$, the gate–channel Schottky junction diode $I_g(V_{\rm gs})$, and the gate–source capacitance $C_{\rm gs}(V_{\rm gs}, V_{\rm ds})$ [25].

The Hermite rationals adopted use a fifth-degree polynomial numerator and fourth-degree polynomial denominator for the hyperbolic tangent that models $I_{\rm ds}(V_{\rm ds})$ behavior; and a tenth-degree polynomial numerator and ninth-degree polynomial denominator for the other nonlinearities [25].

In Figs. 1 and 2, comparisons between the analytical model [25] and the rational approximant are given for the functions and their first three derivatives.

As can be seen, the approximation of an analytical model by Hermite rationals is a very good choice since it accurately interpolates the function and its derivatives. If a greater accuracy is needed, more terms in the numerator or denominator polynomials should be used.

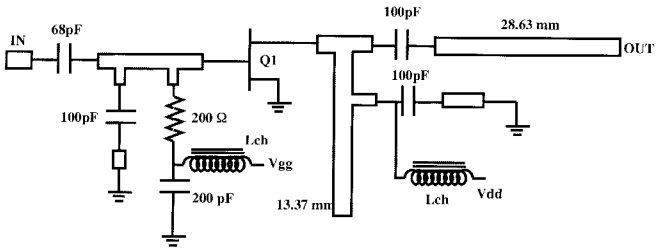

Fig. 3. Schematic diagram of the implemented class-B power-amplifier prototype.

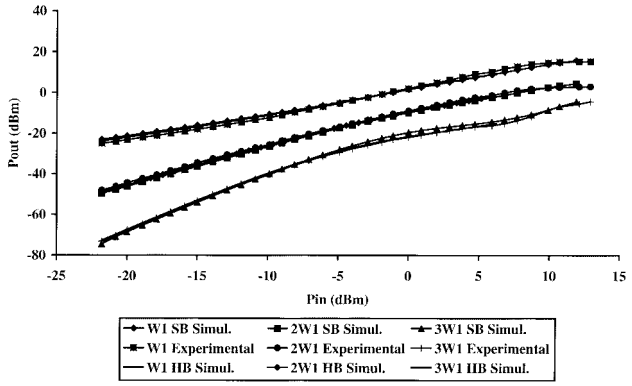

Fig. 4. HB and SB simulated results and experimental results obtained from the one-tone excitation of our class-B power amplifier.

V. Application Examples

In order to validate the proposed ideas, a microwave class-B power-amplifier circuit (see Fig. 3) and a multioctave feedback amplifier were simulated using an in-house developed SB simulator. To prove the fitness of the proposed algorithm to the multitone IMD simulation problem, and the Hermite rational as an adequate nonlinear model approximant, simulated and measured results of single-tone, two-tone, and spectral regrowth obtained from the class-B amplifier are compared.

A. Class-B Power Amplifier

This power-amplifier circuit was excited by four different types of signals:

1) sinusoidal input—one tone;
2) sinusoidal input—two tones;
3) sinusoidal multitone spectra, one carrier amplitude modulated by a pseudorandom sequence;
4) narrow-band discretized flat continuous spectrum with a notch.

1) One-Tone Test: Results of one-tone excitation obtained from a commercial HB package[1] and our SB simulator were compared to the ones measured on the experimental prototype. Fig. 4 reports observed output power levels for the fundamental, second, and third harmonics.

It can be concluded that, for this case, the differences from our SB simulator to MDS or to measured data are within the numerical accuracy.

2) Two-Tone Test: Another classic linearity evaluation, the two-tone IMD test, was performed, again using our SB simulator, HB, and experimental observed results.

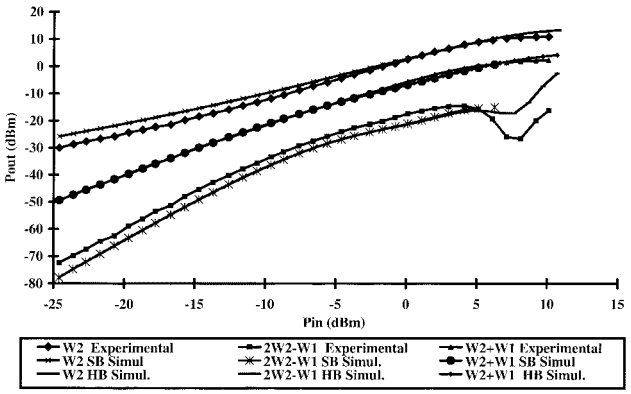

Fig. 5. HB and SB two-tone simulations and experimental results observed in the implemented class-B amplifier.

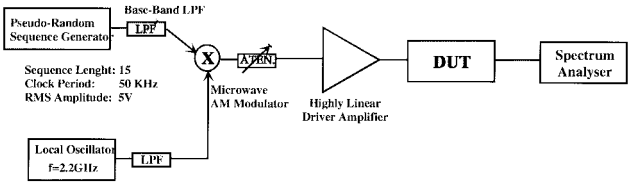

Fig. 6. Setup used for multitone spectral-regrowth tests.

The results are presented on Fig. 5 for one of the fundamentals $\omega 2$ and a second- and third-order products at $\omega_1 + \omega_2$ and $2\omega_2 - \omega_1$.

Although these results are not as good as the previous ones, they can still be considered in very good agreement. It should be noted that although there are some small discrepancies between measured and simulated data, SB and HB results are exactly coincident. This is believed to be due to a slight imperfection during the active-device-model extraction procedure.

3) Spectral-Regrowth Test: For predicting spectral-regrowth behavior, a single carrier modulated by a baseband pseudorandom sequence was assumed as the input excitation. In the frequency domain, this is a multitone signal composed by a certain number of spectral components centered at the carrier frequency and equally separated by $1/T_L$, where T_L is the sequence-repetition period.

Multitone simulation problems are much more complex, because of the role played by the phase between spectral samples. In the laboratory, the phase between tones was obtained by sampling the baseband signal with a digitizing oscilloscope. Knowing that this multitone signal can be considered a very narrow excitation compared with the setup's bandwidth, we assumed that the relative spectral samples' phases are constant throughout the driving circuit.

The adjustable baseband low-pass filter represented in the block diagram of Fig. 6 was intended to control the number of simultaneous driving tones. The input-signal spectrum is presented in Fig. 7.

Although the calculations determined components' values until the fifth harmonic, only the output fundamental and its associated third- and fifth-order spectral regrowth were plotted in Fig. 8.

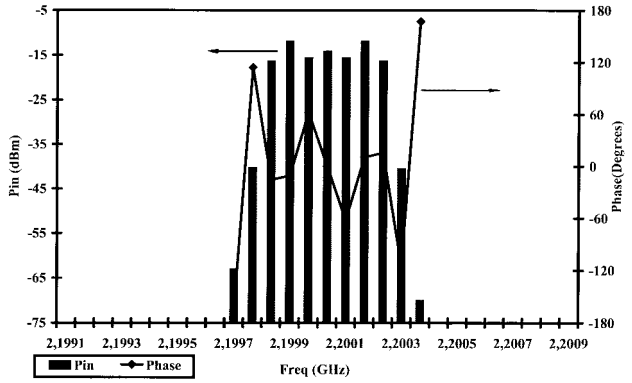

Fig. 7. Input-signal spectrum used for multitone spectral-regrowth tests.

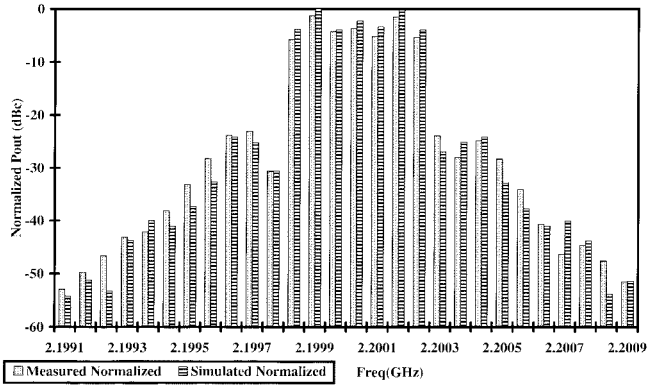

Fig. 8. SB simulated and measured output spectrum obtained from a multitone spectral-regrowth test.

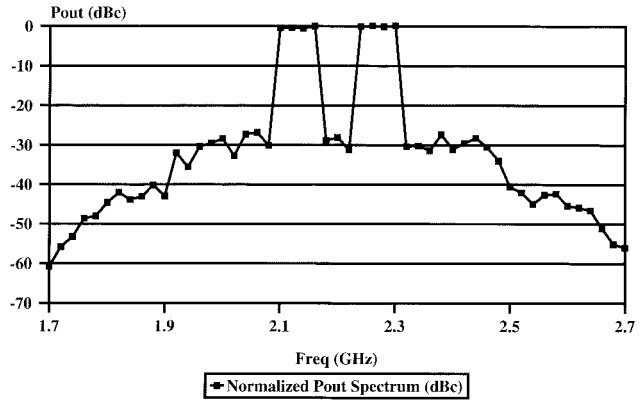

Fig. 9. Output results of the simulated NPR test performed on the class-B amplifier prototype.

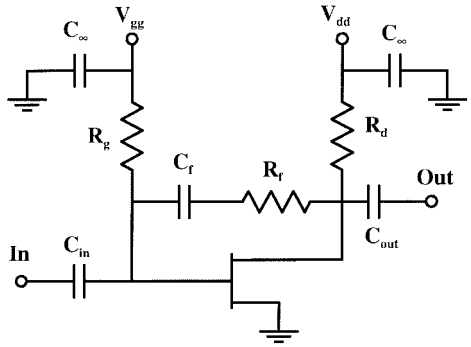

Fig. 10. Simplified schematic diagram of single-stage transimpedance amplifier.

By comparing these simulated and experimental results, it can be easily concluded that our simulator gives a very good prediction of the real power-amplifier behavior when it is excited by a single sinusoid, a two-tone, or even multitone signals. In this case, the simulated input signal was an A.M.-modulated carrier, but since SB algorithm is sensitive to the phases between spectral samples, it is also possible to simulate A.M.–P.M. distortion in more complex modulation schemes.

4) NPR Test: The excitation generally used to perform an NPR test is a continuous spectrum signal with random phase since it is derived from a real noise generator. However, if this laboratory test is to be simulated in a digital computer, i.e., a finite-state machine, some frequency sampling must be used [9]. The most obvious way to do that consists of using a uniform sampling rate, which enables the application of the above derived formulation. Note that if the envelope-type simulation [5], [6] was used for that purpose, uniform sampling of the input and output spectrum was automatically done to enable the presentation of the analysis results in frequency domain. In fact, even if the considered envelope was aperiodic (continuous RF spectrum), the use of the DFT required to perform the domain data translation, immediately produces an envelope repetition (spectral sampling) with a period equal to time-domain simulation duration.

Thus, in order to simulate an NPR test, the circuit of Fig. 3 was excited by a signal consisting of a narrow-band discretized spectrum with a notch that spans from 2.1 to 2.3 GHz. The phase of each of the 11 samples was considered random. Fifteen different random phase arrangements were simulated, and their results averaged. That average result is presented on Fig. 9.

As was expected, some distortion components appeared between the two input noise bands. The ratio between the output fundamental signal level and these distortion components (about 28 dBc) gives a measure of the NPR figure-of-merit for this power amplifier.

B. Multioctave Amplifier

To prove the application of SB to multioctave bandwidth circuits, a single-stage feedback transimpedance amplifier, intended for an optical-fiber TV distribution system, was used (see Fig. 10).

The simulation of this circuit assumed an input signal consisting of 32 tones (see Fig. 11) representing 32 channels. The first channel stands at 46 MHz and the last at 759 MHz. Different power levels were assigned to each channel for better representation of a real situation. As is shown in Fig. 11, four of the channels were shut off to allow correct identification of the generated spurious signals.

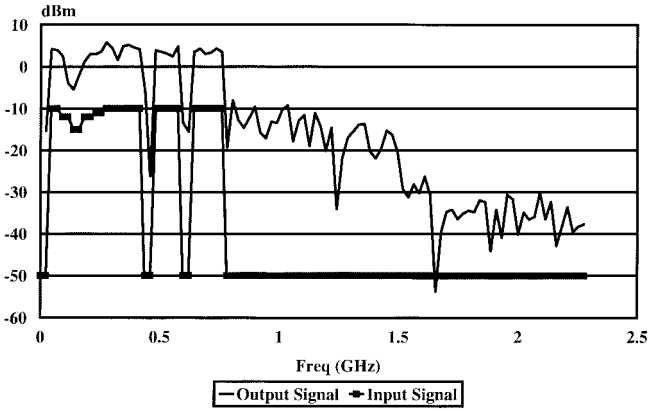

Fig. 11. Input (.) and output (-) signal spectrum of transimpedance amplifier.

As can be seen from Fig. 11, the amplifier produces a distortion level that significantly disturbs the output linear signal components. That is because the amplifier was deliberately hard driven in order to subject the nonlinear simulator to a strong large-signal regime. To our knowledge, this is the first time that a multitone very wide-bandwidth nonlinear circuit driven into saturation is simulated. This proves that SB techniques associated with the indexing vector now proposed can be efficiently used to solve this type of (until now, uncovered) simulation problem.

VI. Conclusions

In this paper, new frequency indexing technique and convolution-matrix generation, were presented. With this novel index technique, computer-simulation time and memory requirements could be relaxed (our simulator prototype run on a PC), which enabled us to apply the SB algorithm to otherwise almost untreatable driving signals, e.g., excitations composed of a large number of tones or, in general, any uniformly discretized spectrum.

On the other hand, since the proposed convolution-matrix generation algorithm can be used with any index frequency vector (and is, to our opinion, more intuitive than the ones previously published), this work can perfectly integrate all the other cases already addressed. In fact, when the input-signal spectrum is not regular, the heavy index-vector generation algorithm proposed by Steer [14] has to be used. However, if that spectrum includes a large number of equally spaced tones (or tones which can be transformed into that), then one should take advantage of this symmetry by using the now proposed index-vector generation algorithm.

Moreover, a new way to approximate analytical or tabular nonlinear models using Hermite rationals was proposed. Since Hermite rationals use information about the function and its derivatives, it becomes possible to simultaneously simulate small- and large-signal behavior.

References

[1] L. W. Nagel, "Spice 2: A computer program to simulate semiconductor circuits," Memo ERL-M520, Electron. Res. Lab., Univ. California, Berkeley, 1975.

[2] M. S. Nakhla and J. Vlach, "A piecewise harmonic balance technique for determination of periodic response of nonlinear systems," *IEEE Trans. Circuits Syst.*, vol. CAS-23, pp. 85–91, Feb. 1976.

[3] V. Rizzoli, C. Cecchetti, and A. Lipparini, "A general-purpose program for the analysis of nonlinear microwave circuits under multi-tone excitation by multidimensional Fourier transform," in *17th European Microwave Conf.*, Rome, Italy, Sept. 1987, pp. 635–640.

[4] L. O. Chua and A. Ushida, "Algorithms for computing almost periodic steady-state response of nonlinear systems to multiple input frequencies," *IEEE Trans. Circuits Syst.*, vol. CAS-28, pp. 953–971, Oct. 1981.

[5] A. Howard, "Circuit envelope simulator analyzes high-frequency modulated signals," *RF Design*, pp. 36–45, Sept. 1995.

[6] E. Ngoya and R. Larchevèque, "Envelope transient analysis: A new method for the transient and steady state analysis of microwave communication circuits and systems," in *IEEE Microwave Theory Tech. Symp. Dig.*, San Francisco, CA, June 18–20, 1996, pp. 1365–1368.

[7] S. Maas, *Nonlinear Microwave Circuits.* Norwood, MA: Artech House, 1988.

[8] M. B. Steer and P. J. Khan, "An algebraic formula for the output of a system with large-signal, multifrequency excitation," *Proc. IEEE*, vol. 71, pp. 177–179, Jan. 1983.

[9] S. A. Maas, "Volterra analysis of spectral regrowth," *IEEE Microwave Guided Wave Lett.*, vol. 7, pp. 192–193, July 1997.

[10] ———, "How to model intermodulation distortion," in *IEEE Microwave Theory Tech. Symp. Dig.*, Boston, MA, 1991, pp. 149–151.

[11] V. Rizzoli and A. Neri, "State of the art and present trends in nonlinear microwave CAD techniques," *IEEE Trans. Microwave Theory Tech.*, vol. 36, pp. 343–364, Feb. 1988.

[12] K. K. M. Cheng and J. K. A. Everard, "Nonlinear circuit analysis using the Newton–Sor continuation method," *Electron. Lett.*, vol. 26, pp. 2120–2121, Dec. 1990.

[13] K. S. Kundert, J. K. White, and A. Sangiovanni-Vicentelli, *Steady-State Methods for Simulating Analog and Microwave Circuits.* Norwell, MA: Kluwer, 1990.

[14] G. W. Rhyne and M. B. Steer, "Frequency-domain nonlinear circuit analysis using a frequency-domain harmonic balance technique," *IEEE Trans. Microwave Theory Tech.*, vol. 36, pp. 379–387, Feb. 1988.

[15] T. Närhi, "Analysis of strongly nonlinear circuits with a frequency-domain method coupled with a consistent large-signal model," in *IEEE Microwave Theory Tech. Symp. Dig.*, Atlanta, GA, 1993, pp. 633–636.

[16] C.-R. Chang, "Computer-aided design of nonlinear microwave analog circuits using frequency-domain spectral balance," Ph.D. dissertation, Dept. Elect. Computer Eng., North Carolina State Univ., Raleigh, NC, Oct. 1990.

[17] T. Närhi, "Frequency-domain analysis of strongly nonlinear circuits using a consistent large-signal model," *IEEE Trans. Microwave Theory Tech.*, vol. 44, pp. 182–192, Feb. 1996.

[18] C.-R. Chang, M. B. Steer, and G. W. Rhyne, "Frequency-domain spectral balance using the arithmetic operator method," *IEEE Trans. Microwave Theory Tech.*, vol. 37, pp. 1681–1688, Nov. 1989.

[19] M. B. Steer, C.-R. Chang, and G. W. Rhyne, "Computer-aided analysis of nonlinear microwave circuits using frequency-domain nonlinear analysis techniques: The state of the art," *Int. J. Microwave Millimeter-Wave Computer-Aided Eng.*, vol. 1, no. 2, pp. 181–200, 1991.

[20] E. Van den Eijnde, "Steady-state analysis of strongly nonlinear circuits," Ph.D. dissertation, Dept. ELEC, Vrije Universiteit Brussel, Brussels, Belguim, 1989.

[21] E. Van Den Eijnde and J. Schoukens, "Steady state analysis of a periodically excited nonlinear systems," *IEEE Trans. Circuits Syst.*, vol. 37, pp. 232–242, Feb. 1990.

[22] E. Ngoya, J. Rousset, M. Gayral, R. Quere, and J. Obregon, "Efficient algorithms for spectra calculations in nonlinear microwave circuits simulators," *IEEE Trans. Circuits Syst.*, vol. 37, pp. 1339–1355, Nov. 1990.

[23] A. Cuyt and L. Wuytack, *Nonlinear Methods in Numerical Analysis* (Mathematics Studies Series 136). Amsterdam, The Netherlands: North-Holland, 1991.

[24] A. Cuyt and B. Verdonk, "Multivariate rational interpolation," *Computing*, vol. 34, pp. 41–61, 1985.

[25] J. C. Pedro and J. Perez, "A novel nonlinear GaAs FET model for intermodulation analysis in general purpose harmonic balance simulators," in *23rd European Microwave Conf.*, Madrid, Spain, 1993, pp. 714–716.

Nuno Borges de Carvalho (S'92) was born in Luanda, Angola, on April 29, 1972. He received the diploma degree in electronics and telecommunications engineering from the University of Aveiro, Aveiro, Portugal, in 1995, and is currently working toward the Ph.D. degree.

In 1997, he was appointed Assistant Lecturer at the University of Aveiro. His research interests include CAD for nonlinear circuits and active device modeling and design, mainly for power amplifiers.

Mr. Carvalho is a member of the Portuguese Engineering Association. He was the recipient of the 1995 Best Engineer Student Award presented by the University of Aveiro. He also received the Portuguese Engineering Association Prize as the best 1995 student at the University of Aveiro.

José Carlos Pedro (S'90–M'95) was born in Espinho, Portugal, on March 7, 1962. He received the diploma and doctoral degrees in electronics and telecommunications engineering, from the University of Aveiro, Aveiro, Portugal, in 1985 and 1993, respectively.

From 1985 to 1993, he was an Assistant Lecturer at the University of Aveiro, was appointed a Professor in 1993, and is currently an Associate Professor. He also works with the Telecommunications Institute as a Senior Research Scientist. His main scientific interests include active device modeling, and the analysis and design of various nonlinear microwave and optoelectronics circuits, in particular, the design of highly linear multicarrier power amplifiers.

Dr. Pedro received the Marconi Young Scientist Award in 1993.